

Turbulent wall jets

V. KUPPU RAO AND M. INDERJIT

Department of Mechanical Engineering, Indian Institute of Science, Bangalore 560 012

Received on April 26, 1977; Revised on November 4, 1977

Abstract

Similarity analyses of the governing equations of three types of turbulent wall jet—the Radial Wall Jet, the Plane Wall Jet and one that is referred to as the Spherical Wall Jet—are developed. The analyses indicate how self-preserving flow can obtain in all the three cases. The Radial Wall Jet and the Plane Wall Jet have been investigated extensively and are reported to possess self-preserving flow. In the present case, a large number of mean velocity measurements have been taken in the fully developed region of turbulent Spherical Wall Jets. Some of these velocity profiles are presented here and are seen to exhibit similarity.

1. Introduction

The turbulent wall jets that develop on plane surfaces when a jet of fluid impinges on them have been studied extensively. In particular, two types of wall jet have received great attention; one, usually called the Radial Wall Jet, is the flow that develops on a plane surface against which a small circular jet of fluid impinges normally and, the other, usually called the Plane Wall Jet, is the flow that develops over a plane surface which is placed parallel to a narrow slot from which a two-dimensional fluid jet emerges. In both cases, it has been observed that the velocity profiles in the fully developed regions of the wall jet are 'self-preserving' and are geometrically similar at stations beyond a short development region.^{1, 2}

In the following, an attempt has been made to extend the study to the axisymmetric wall jet that develops on a spherical surface when a small circular fluid jet impinges on it radially. This will be referred to as the Spherical Wall Jet. The study is confined to cases where the diameter of the spherical surface is large compared to the jet diameter so that the equations of motion can be simplified with the boundary-layer approximations. First, a simple similarity analysis is presented for fully developed flow for each of the three cases, the Radial Wall Jet, the Plane Wall Jet and the Spherical Wall Jet. The analysis brings out certain requirements for each case in order that the velocity profiles are self-preserving. The results of a large number of mean velocity measurements in Spherical Wall Jets are then presented.

2. Similarity analysis*

Fig. 1 shows a typical 'self-preserving' velocity profiles in a wall jet. Region (a) in which the velocity increases from zero at the surface to U , the maximum value at that section, has been compared to a two-dimensional boundary layer in a uniform stream by some authors and may be called the inner layer. Region (b) where the velocity decreases from U to zero in the free boundary asymptotically may be compared to a free jet and called the outer layer. It is difficult to define exactly the thickness of the outer layer and, consequently, the thickness of the wall jet itself. We may arbitrarily define the thickness δ of the wall jet at any location as the distance from the surface at which the velocity u has decreased to one half of U , the maximum velocity at that section as indicated in Fig. 1.

2.1. The radial wall jet

We now consider the fully developed region of flow in a turbulent Radial Wall Jet with self-preserving velocity profiles. Assuming steady, incompressible flow and introducing the boundary layer approximations, the governing equations can be written, with the usual notation, as:

$$\frac{\partial}{\partial x} (xu) + \frac{\partial}{\partial y} (xv) = 0 \quad \text{Continuity equation}$$

$$u \frac{\partial u}{\partial x} + v \frac{\partial u}{\partial y} = \frac{\partial}{\partial y} \left(\frac{\tau}{\rho} \right) \quad \text{Momentum equation}$$

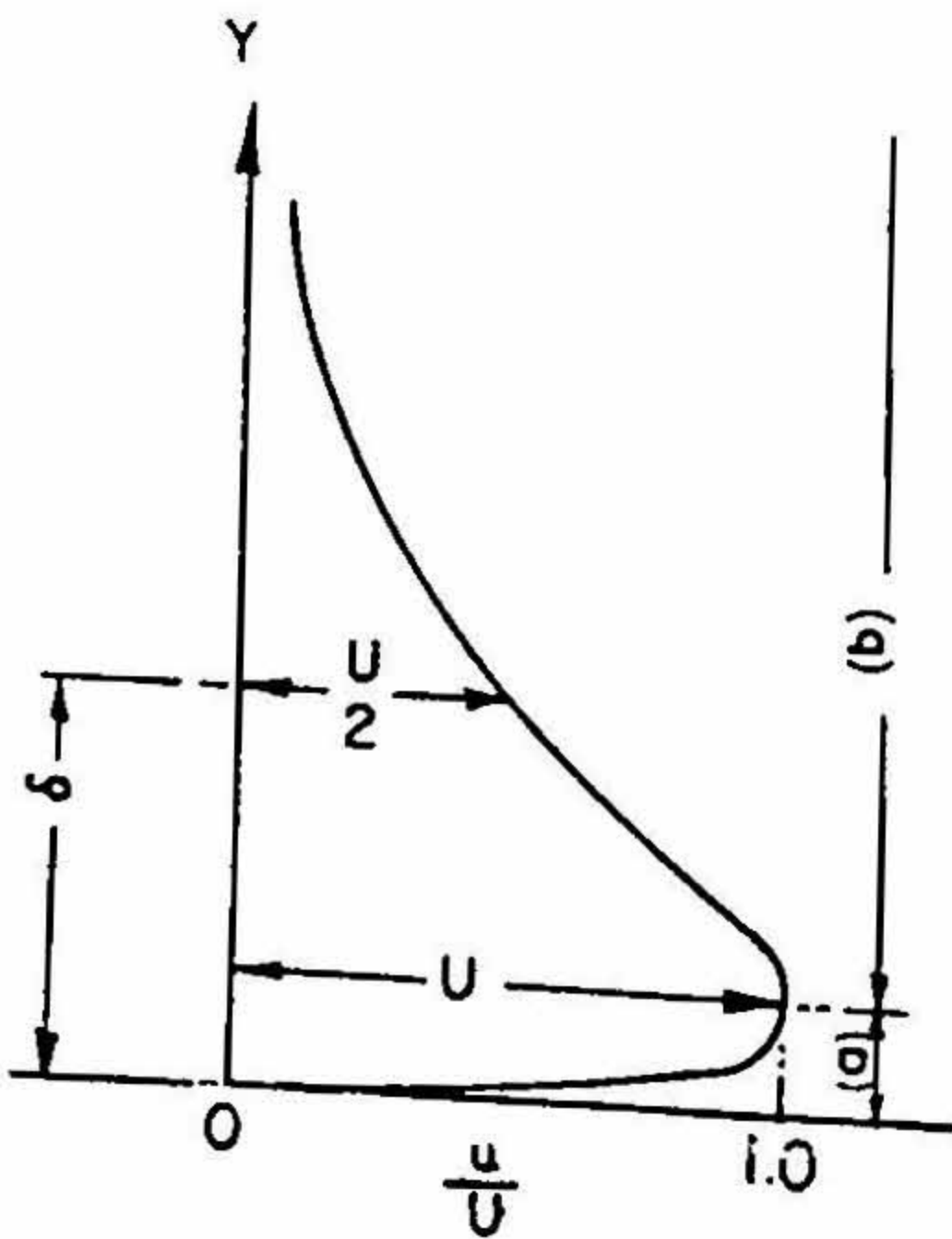


FIG 1

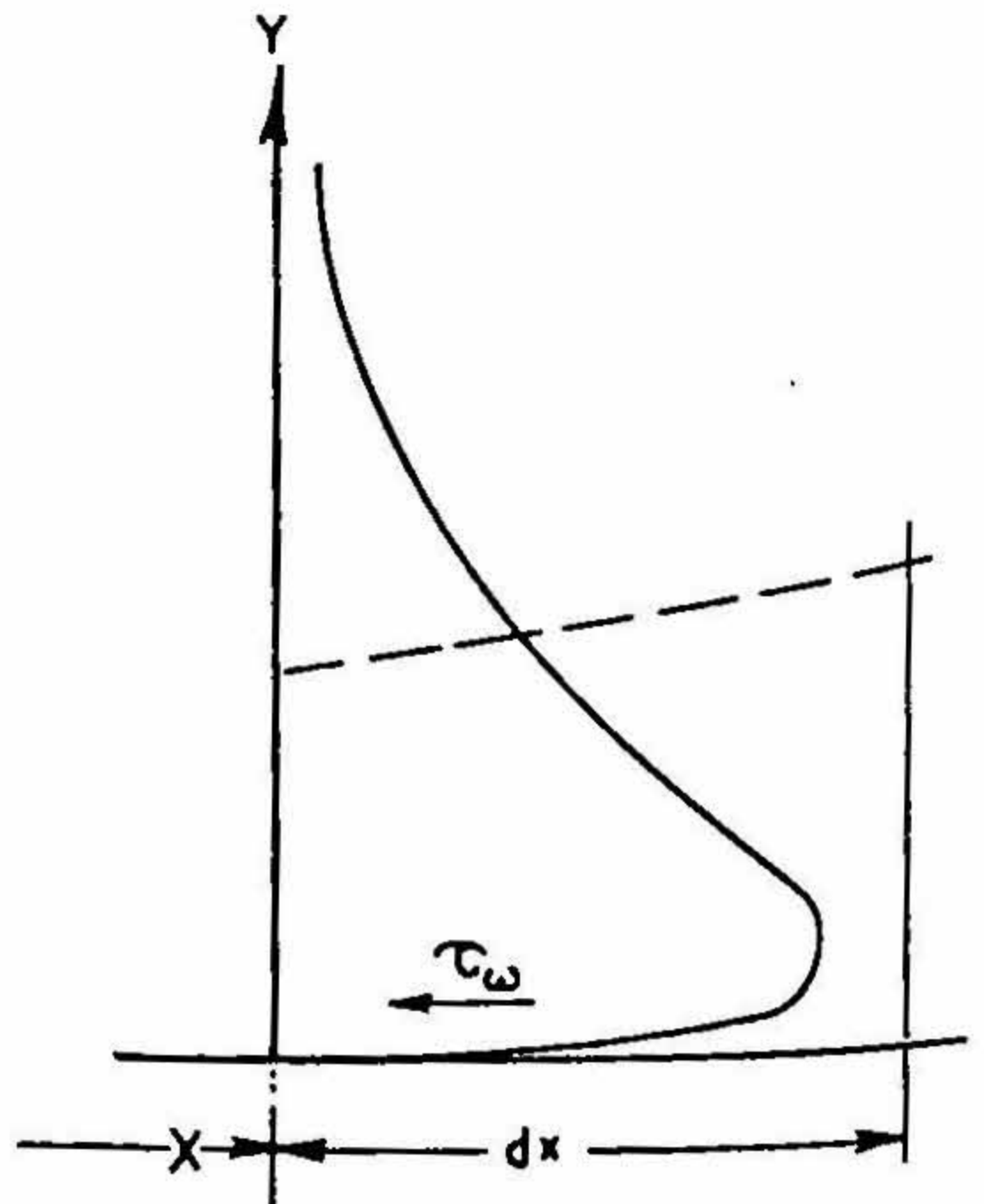


FIG. 2

* A similarity analysis for wall jets very similar to the one developed here is presented in ref. 8. However, when the authors evolved this analysis, ref. 8 had not yet been published.

where u and v are the mean velocities in the streamwise (x) and the transverse (y) directions respectively.

Now,

$$\frac{\tau}{\rho} = \nu \frac{\partial u}{\partial y} - \overline{u'v'}$$

where u' and v' are instantaneous fluctuations in u and v . Near the solid boundary, the turbulent fluctuations die down and molecular diffusion of momentum predominates over turbulent diffusion. As one moves away from the solid boundary, the contribution of turbulent diffusion increases very rapidly until, at a small distance away from the wall, molecular diffusion can be neglected completely. If δ_s is the thickness of the layer beyond which molecular diffusion is negligible, then,³

$$\frac{\delta_s \cdot u^*}{\nu} \approx 60.$$

However, the thickness of the layer in which the shear stress is constant (and equal to that at the wall) is very much more than this. One may therefore substitute $\tau/\rho = -\overline{u'v'}$ from the edge of the constant shear layer to the wall and thus for the entire boundary layer so that the momentum equation can be written as:

$$u \frac{\partial u}{\partial x} + v \frac{\partial u}{\partial y} = - \frac{\partial}{\partial y} \overline{u'v'}$$

We now seek a similarity solution of these equations by introducing the following:

1. Power law variation for the wall jet thickness δ and the maximum velocity at any section U given by:

$$U = Ax^a ; \quad \delta = Bx^b$$

x being measured from a 'virtual origin' not necessarily coincident with the stagnation point on the surface.

2. A similarity parameter $\eta = y/\delta = y/Bx^b$.
3. The self-preserving velocity profile $u/U = f(\eta)$.
4. Representation of the Reynolds Stresses as $\overline{u'v'} = U^2 \cdot h(\eta)$.

The continuity equation is eliminated by introducing the stream function ψ such that

$$u = \frac{1}{x} \cdot \frac{\partial \psi}{\partial y} ; \quad v = - \frac{1}{x} \cdot \frac{\partial \psi}{\partial x}$$

The stream function at any section x is then:

$$\psi = \int_0^y x u dy = ABx^{a+b+1} \int_0^\eta f(\eta) \cdot d\eta = ABx^{a+b+1} \cdot F(\eta),$$

where

$$F(\eta) = \int_0^\eta f(\eta) \cdot d\eta.$$

With these substitutions, the momentum equation turns out as:

$$A^2 a x^{2a-1} \cdot F'^2 - A^2 (a+b+1) x^{2a-1} \cdot FF'' = -\frac{A^2}{B} \cdot x^{2a-b} \cdot h'$$

where the primes indicate differentiation with respect to η .

For similarity, therefore, $b = 1$.

To evaluate the index a , let us consider the Momentum-Integral equation of the Radial Wall Jet. Referring to Fig. 2, this equation can be written as:

$$\frac{d}{dx} \int_0^\infty u^2 \cdot x \cdot dy + \frac{\tau\omega}{\rho} x = 0.$$

which integrates to:

$$\int_0^\infty u^2 x dy + \int_0^x \frac{\tau\omega}{\rho} x dx = \text{Constant},$$

or, with the present substitutions,

$$A^2 B x^{2a+b+1} \int_0^\infty F'^2 \cdot d\eta - A^2 h(0) \int_0^x x^{2a} \cdot dx = \text{Constant}$$

This equation is equivalent to: Momentum flow/unit time at any section x + Wall shear force retarding the flow up to that section = Constant = Momentum/unit time added to the flow by the impinging jet.

In Free Jets where the mean velocity profiles are self-preserving, the momentum of the jet fluid is conserved at all sections. This is not so in the case of wall jets because of loss of momentum at the solid boundary. However, one is forced to neglect this if one hopes to complete the similarity analyses. It may be noted that the ratio of the momentum loss to the total momentum of the jet fluid will be of the order of 10^{-2} . The analyses will, therefore, be inaccurate to this extent and can be expected to predict the gross features of these flows rather than their finer details.

If we neglect, therefore, the second term on the L.H.S. of the Momentum-Integral relation, we see that:

$$2a + b + 1 = 0$$

or,

$$a = -1.$$

The momentum equation simplifies then to:

$$F'^2 + FF'' - \frac{h'}{B} = 0 \quad (1)$$

with the boundary conditions:

$$\eta = 0: F = 0, \quad F' = 0;$$

$$\eta \rightarrow \infty: F' \rightarrow 0.$$

2.2. The plane wall jet

The governing equations are:

$$\frac{\partial u}{\partial x} + \frac{\partial v}{\partial y} = 0 \quad \text{Continuity equation}$$

$$u \frac{\partial u}{\partial x} + v \frac{\partial u}{\partial y} = - \frac{\partial}{\partial y} \overline{u'v'} \quad \text{Momentum equation.}$$

The stream function at any section x is now $\psi = \int u \cdot dy$ and we introduce the same substitutions as before to transform the momentum equation to:

$$A^2 ax^{2a-1} \cdot F'^2 - A^2(a+b)x^{2a-1} \cdot FF'' = - \frac{A^2}{B} \cdot x^{2a-b} \cdot h'.$$

For similarity, again, $b = 1$.

The momentum-integral equation is now

$$\frac{d}{dx} \int_0^{\infty} u^2 \cdot dy + \frac{\tau\omega}{\rho} = 0$$

which integrates to:

$$\int_0^{\infty} u^2 \cdot dy + \int_0^x \frac{\tau\omega}{\rho} \cdot dx = \text{Constant.}$$

or,

$$A^2 B \cdot x^{2a+b} \int_0^\infty F'^2 \cdot d\eta + \int_0^x \frac{\tau\omega}{\rho} \cdot dx = \text{Constant.}$$

In this case, therefore, $2a + b = 0$ or $a = -\frac{1}{2}$.

The momentum equation simplifies to:

$$F'^2 + FF'' - \frac{2h'}{B} = 0 \tag{2}$$

with the same boundary conditions as for equation (1).

These values of a and b obtained for the two types of wall jet from the present analysis are compared with their experimental values reported in literature⁴ in the table below

	Radial Wall Jet		Plane Wall Jet	
	Present Analysis	Reported	Present Analysis	Reported
a	-1.0	-1.12	-0.5	-0.555
b	1.0	0.94	1.0	1.0

2.3. The spherical wall jet

Assuming that the diameter of the circular jet impinging on the sphere is small compared to the sphere diameter (so that the thickness of the resulting wall jet is small), we can write the governing equations as (with reference to Fig. 3):

$$\frac{\partial}{\partial x}(ur) + \frac{\partial}{\partial y}(vr) = 0 \quad \text{Continuity equation}$$

$$u \frac{\partial u}{\partial x} + v \frac{\partial u}{\partial y} = \frac{\partial}{\partial y} \left(\frac{\tau}{\rho} \right) \quad \text{Momentum equation.}$$

We now introduce substitutions similar to those that were introduced earlier with the essential difference that, in the present case, r replaces x in the similarity transformations so that:

$$U = Ar^a,$$

$$\delta = Br^b,$$

$$\eta = y/\delta = y/Br^b,$$

$$u = U \cdot f(\eta) = \frac{1}{r} \cdot \frac{\partial \psi}{\partial y}; \quad v = -\frac{1}{r} \cdot \frac{\partial \psi}{\partial x},$$

$$\psi = AB r^{a+b+1} \int f(\eta) \cdot d\eta = AB r^{a+b+1} \cdot F(\eta)$$

Further, we now write the shear force term in the momentum equation as:

$$\frac{\partial}{\partial y} \left(\frac{\tau}{\rho} \right) = \varepsilon \cdot \frac{\partial^2 u}{\partial y^2} = (\varepsilon_0 \cdot \cos \theta) \cdot \frac{\partial^2 u}{\partial y^2}$$

where ε is the 'eddy viscosity' at any section and ε_0 is its value at the stagnation point $\theta = 0$. This substitution, though artificial and highly contrived, is essential for similarity. It implies that the shear stress vanishes at $\theta = 90^\circ$. This may be true of the wall shear stress τ_w as the wall jet appears to leave the surface at $\theta = 90^\circ$. There is no justification *a priori* for this substitution; it can only be defended, *a posteriori*, from the similarity trend shown by the velocity profiles in the developed region of the Spherical Wall Jet.

With these substitutions, the momentum equation transforms to:

$$\begin{aligned} A^2 ar^{2a-1} \cdot F'^2 \cos \theta - A^2 (a+b+1) r^{2a-1} \cdot FF'' \cos \theta \\ = \varepsilon_0 \cdot \frac{A}{B^2} \cdot r^{2a-b} F''' \cos \theta \end{aligned}$$

The Momentum-Integral relation indicates $2a + b + 1 = 0$. These result in values for a and b of -1 and 1 respectively and the momentum equation simplifies to:

$$F'^2 + FF'' + \left(\frac{\varepsilon_0}{AB^2} \right) F''' = 0 \quad (3)$$

with the same boundary conditions as for equations (1) and (2).

3. Numerical solution

The three equations, (1), (2) and (3) can be integrated by standard numerical methods. Before this is done, however, in equations (1) and (2), the function $h(\eta)$ used to represent the Reynolds Stress distribution has to be connected with the function F and its derivatives by invoking some theory of turbulent diffusion. In equation (3) with which we are now primarily concerned, the variation of ε_0 with y (and hence η) will again depend on the particular hypothesis of turbulent diffusion that is assumed. It is also likely that different empirical hypotheses may be appropriate for the inner and the outer layers of the wall jet. This is because, in the outer layer, diffusion by large eddies (as in free jets) may predominate, whereas, in the highly sheared inner layer, velocity gradients and small eddies may control diffusion.

In the present instance, for purposes of illustration, ϵ_0 has been assumed constant and equation (3) has been written as

$$F'^2 + FF'' + CF''' = 0 \quad [C = \text{Constant}] \quad (4)$$

and numerically integrated by the Runge-Kutta method.

The shape of the velocity distribution curve (F') that results by integrating equation (4) can be varied by (a) varying the value of the constant C and (b) varying $F''(0)$ $[(\partial u/\partial y)_{y=0}]$, the velocity gradient at the surface specified at the start of the numerical integration process. No attempt was made to incorporate the other classical theories of turbulent diffusion as all are of dubious validity.

4. Experimental results

The present set of experiments was confined mainly to the Spherical Wall Jet as the other two types have been investigated extensively.^{1,2,5-7} The Spherical Wall Jet was produced by a small circular air jet striking a large spherical surface radially. A rotary compressor supplied the air to the jet nozzle through a large reservoir to minimise pressure fluctuations. Mean velocities at different locations were measured by a small flattened pitot tube 0.2 mm thick and a projection manometer with an accuracy of 0.1 mm.

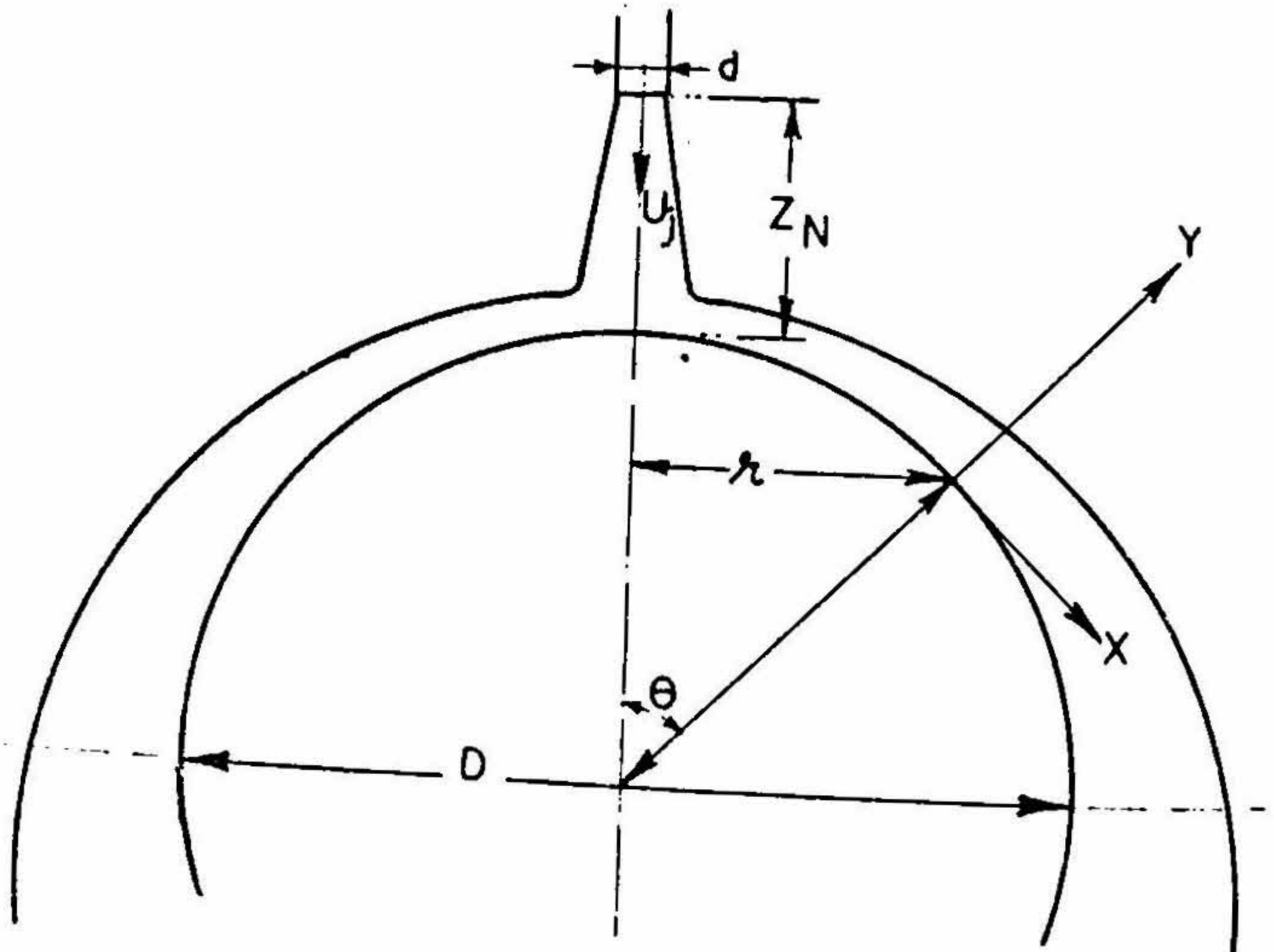


Fig. 3

A jet nozzle of 12.7 mm (0.5") diameter (d) was used in the experiments. The parameters varied were (with reference to Fig. 3):

- (a) The sphere diameter D ,
- (b) The distance between the nozzle and the sphere Z_N and
- (c) The jet exit Reynolds number $Re_j = \frac{U_j \cdot d}{\nu}$

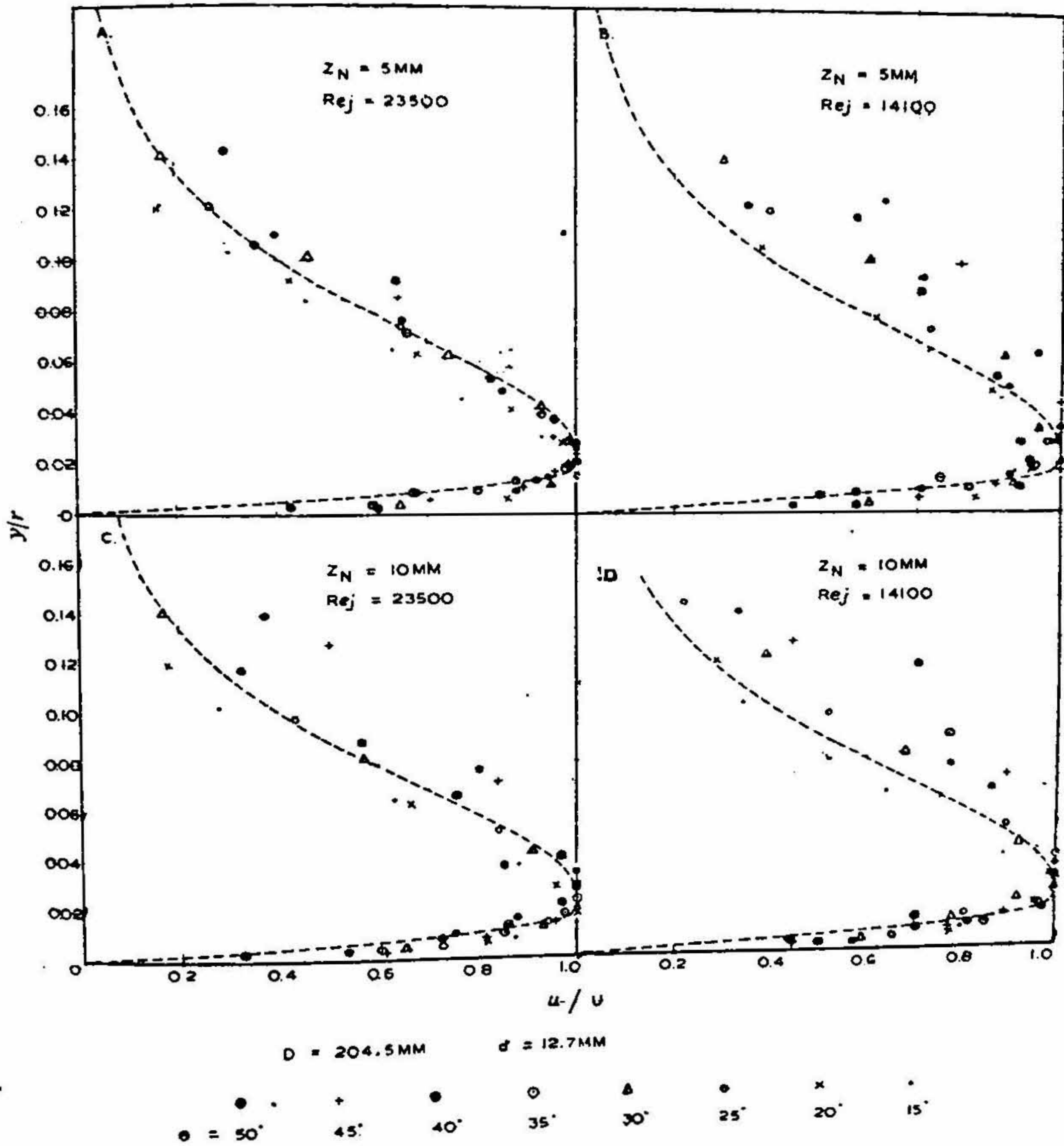


FIG. 4

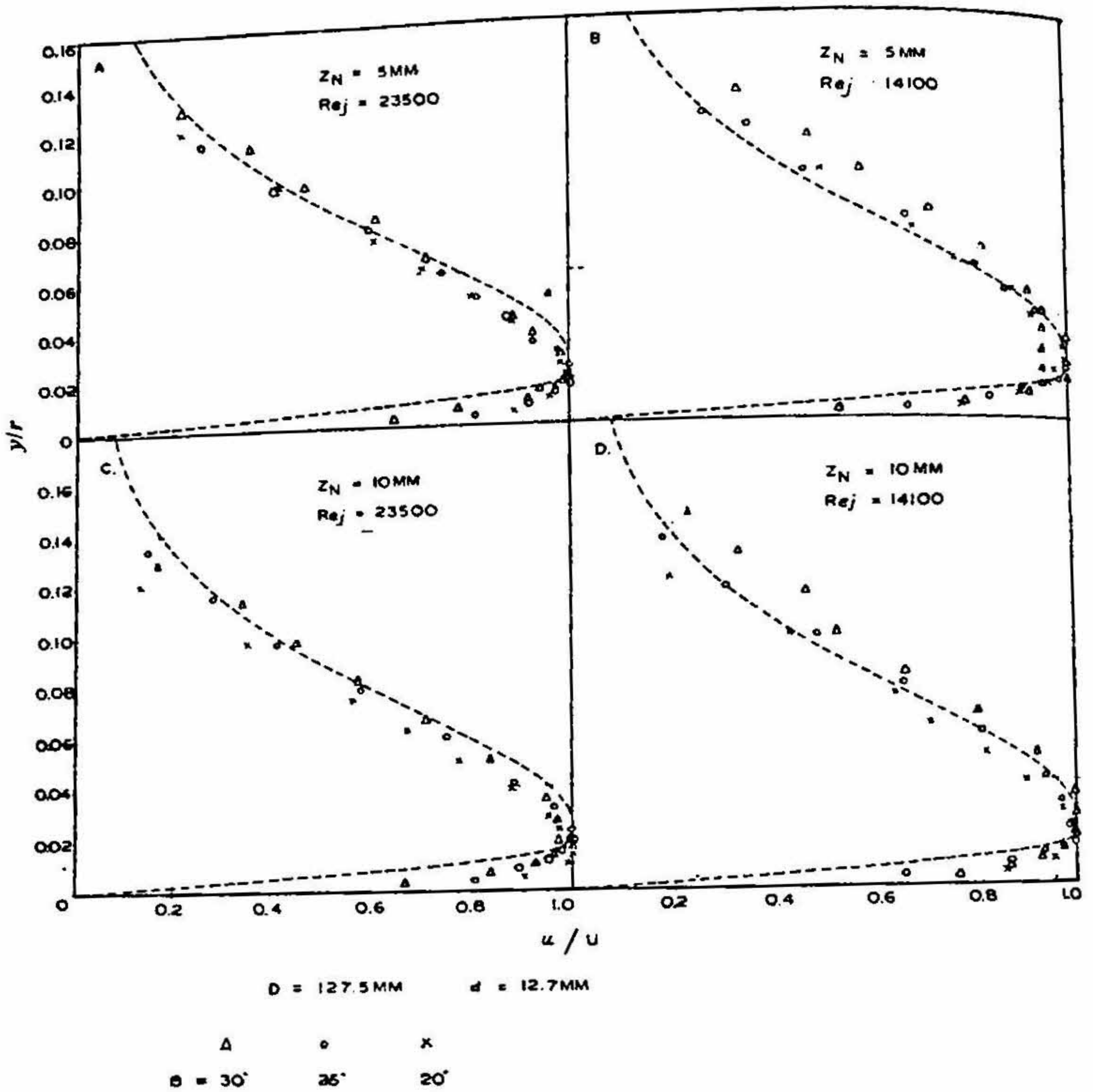


FIG. 5

Some of the results are presented in Figs. 4, 5 and 6 in the form suggested by the similarity analysis. As can be seen, the velocity profiles do exhibit similarity and seem to be little affected by the variation in the three parameters cited above.

The curve shown in broken line in each of these figures was obtained by numerical integration of equation (4) with

(a) $F''(0) = 7.8$ and $C = 0.015$ in the inner layer and

(b) $C = 0.36$ in the outer layer.

5. COSART, W. P AND SCHWARZ, W. H. *J. Fluid Mech.*, 1961, 10, 481.
6. CERMAK, J. E., POREH, M. AND TSUEI, Y. G. *J. Appl. Mech.*, 1967, 34 (2), 457.
7. GAUNTNER, W. J., HRYCAK, P. AND LIVINGOOD, J. B. *NASA TND—5652*, 1970.
8. RAJARATNAM, N. *Turbulent Jets*, 1976, Elsevier Scientific Publishing Company, Amsterdam.